Molecular Vision 2020; 26:345-354 <http://www.molvis.org/molvis/v26/345>
Received 19 February 2020 | Accepted 30 April 2020 | Published 2 May 2020

Clinical, histopathological, and in silico pathogenicity analyses in a pedigree with familial amyloidosis of the Finnish type (Meretoja syndrome) caused by a novel gelsolin mutation

Jesus Cabral-Macias,[1] Leopoldo A. Garcia-Montaño,[2] Mario Pérezpeña-Díazconti,[3] Marisa-Cruz Aguilar,[2] Guillermo Garcia,[1] Carlos I. Vencedor-Meraz,[4] Enrique O. Graue-Hernandez,[1] Oscar F. Chacón-Camacho,[2,5] Juan C. Zenteno[2,6]

[1]Department of Cornea, Institute of Ophthalmology "Conde de Valenciana," Mexico City, Mexico; [2]Research Unit, Institute of Ophthalmology "Conde de Valenciana," Mexico City, Mexico; [3]Pathology Department, Institute of Ophthalmology "Conde de Valenciana," Mexico City, Mexico; [4]Vector Borne Disease Program, Secretaría de Salud Pública, Hermosillo, Sonora, Mexico; [5]Carrera de Médico Cirujano, Facultad de Estudios Superiores Iztacala, Universidad Nacional Autónoma de México, Tlalnepantla, Estado de México, Mexico; [6]Department of Biochemistry, Faculty of Medicine, UNAM, Mexico City, Mexico

Purpose: Familial amyloidosis of the Finnish type (FAF) is an inherited amyloidosis arising from mutations in the gelsolin protein (GSN). The disease includes facial paralysis, loose skin, and lattice corneal dystrophy. To date, FAF has been invariably associated with substitution of Asp214 in GSN. We describe the clinical, histopathological, and genetic features of a family with FAF due to a novel GSN mutation.

Methods: Five affected adult individuals in a three-generation FAF pedigree were included in the study. Histopathological analysis was performed on an eyelid skin biopsy from one patient. Genetic analysis included next-generation sequencing (NGS) and Sanger sequencing for confirmation of the *GSN* variant. Several tools for in silico analysis of pathogenicity for the novel variant and to predict the effect of the amino acid replacement on protein stability were used.

Results: Three older adult affected patients exhibited corneal lattice dystrophy, cutis laxa, and facultative peripheral neuropathy. Two younger adult individuals presented only with corneal amyloid deposits. NGS identified a heterozygous *GSN* c.1631T>G transversion, predicting a novel p.Met544Arg mutation. All in silico tools indicated that p.Met544Arg is deleterious for GSN functionality or stability.

Conclusions: The results expand the molecular spectrum of GSN-linked systemic amyloidosis. The novel p.Met544Arg pathogenic variant is predicted to affect gelsolin function, presumably by impairing a potential calcium-sensitive, actin-binding region.

The term amyloidosis encompasses a heterogeneous group of inherited or sporadic disorders characterized by the progressive aggregation of amyloid protein into various body tissues [1]. Abnormal amyloid deposition in the cornea leads to lattice corneal dystrophy (LCD; OMIM 122200), an eye-limited genetic disorder caused by dominant mutations in the *TGFBI* gene (Gene ID: 7045; OMIM 601692) located at chromosome 5q31 [2-4]. Familial amyloidosis of the Finnish type (FAF; OMIM 105120), also known as Meretoja syndrome or hereditary gelsolin amyloidosis, is a systemic form of LCD that also affects cranial nerves and skin [5]. This disease was first described by Jouko Meretoja 50 years ago [6] and is one of the most common inherited diseases in Finland where approximately 1,000 individuals are known to be affected [7]. However, the disorder is not exclusive to Finnish heritage, and FAF has been reported in patients from distinct ethnicities [8-24].

FAF is caused by recurrent mutations in gelsolin (*GSN*, Gene ID: 2934; OMIM 137350), a gene located at 9q33.2 and encoding for an actin-binding protein involved in cytoplasmic actin regulation and organization. Of note, all patients with FAF analyzed to date have been demonstrated to carry similar mutations at aspartic acid (Asp) residue 187 (corresponding to residue 214 in the currently used gene transcript) of the GSN protein. The most common mutation (known as Finnish type) leads to an Asp to asparagine (Asn) substitution at residue 214 of the protein (p.Asp214Asn) and is associated with typical clinical presentation and complete penetrance. The p.Asp214Asn variant has been identified in Finnish, American, Dutch, British, Portuguese, Spanish, German, Swedish, Iranian, and Japanese pedigrees [10,13,16,17,19,23]. The Danish type GSN mutation leads to a tyrosine replacement, p.Asp214Tyr. It has been described in Danish, Czech, French, Brazilian, and Korean families, and it is associated with an earlier age of onset and with more severe bulbar dysfunction

Correspondence to: Dr. Juan C. Zenteno, Department of Genetics, Institute of Ophthalmology "Conde de Valenciana." Chimalpopoca 14, Col. Obrera, Cuauhtemoc CP 06800, Mexico City, Mexico. Phone: +(52) 5554421700 ext 3212 email: jczenteno@institutodeoftalmologia.org

when compared with subjects carrying the Finnish variant [7,15,22,25]. The p.Asp214Asn or Tyr replacement eventually leads to the release, polymerization, and deposition of the abnormal degradation of GSN protein throughout the body [5].

The clinical triad of FAF includes progressive bilateral facial paralysis, loose skin (cutis laxa), and lattice corneal dystrophy [7]. In heterozygous patients, clinical manifestations usually appear in early adulthood, toward the third or fourth decade of life. The earliest finding is LCD, characterized by amyloid deposition, recurrent corneal erosions, and progressive visual impairment. *GSN* homozygous patients with FAF present earlier onset and greater severity of clinical findings, and can develop a severe nephrotic syndrome [22,26,27].

Although it is currently clear that FAF is not associated with allelic heterogeneity, molecular analysis of additional pedigrees is warranted as it could allow for the expansion of the genetic spectrum leading to the disease. In addition, identification of novel mutations would permit a better genotype–phenotype correlation. In this work, we describe the results of clinical, histopathological, and genetic analyses of a Mexican FAF pedigree carrying a novel causal mutation in *GSN*. The results expand the spectrum of *GSN* defects leading to hereditary systemic amyloidosis.

METHODS

Clinical examination: Five members of a Mexican mestizo family were ascertained for a study which was approved by the institutional ethics committee at the Institute of Ophthalmology Conde de Valenciana (Mexico City, Mexico). Research protocols adhered to the ARVO Statement on Human Subjects and the tenets of the Declaration of Helsinki. All participants gave written informed consent prior to inclusion in the study. Examination included best-corrected visual acuity determination, slit-lamp inspection, biomicroscopy, funduscopy, and applanation tonometry. Systemic anomalies were investigated by a geneticist. Clinical photographs of the cornea were obtained in all participants.

Skin histopathological analysis: Eyelid skin tissue was obtained during a surgical procedure for blepharochalasis in individual II-5 (Figure 1). The tissue samples were fixed in 10% buffer formaldehyde, dehydrated, and embedded in paraffin. Hematoxylin and eosin and Congo red stains were performed in 0.4-µm-thick sections. A Zeiss Axio Imager Z2 (Carl Zeiss Microscopy GmbH, Jena, Germany) research microscope with the ApoTome.2 digital system was used for the microscopic examination.

Molecular analysis: Genomic DNA was extracted from blood leukocytes of the index case and from four available first-degree relatives with the QIAamp DNA Blood kit (Qiagen, Hilden, following the manufacturer's instructions. For PCR amplification of GSN exons 4 and 12 each 25 µl reaction contained 1X buffer, 200 ng of genomic DNA, 0.2 mM of each deoxynucleotide triphosphate, 2U Taq polymerase, 1

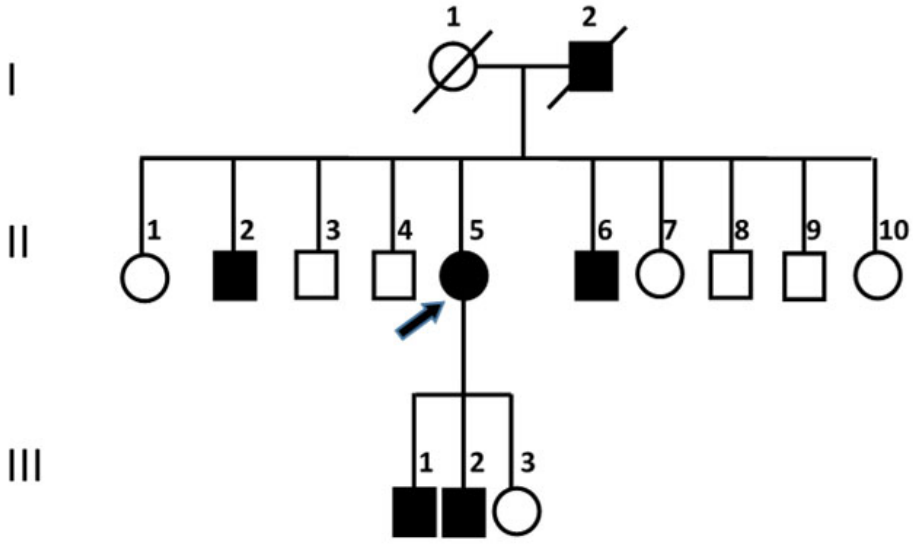

Figure 1. Genealogy of the affected family. Solid symbols indicate affected subjects. Arrow indicates the proband.

Figure 2. Phenotypic appearance of FAF affected subjects. Clinical images of subjects II-2 (**A**), II-5 (**B**), and II-6 (**C**). Cutis laxa, drooping eyelids, and hyperpigmented skin are evident.

mM of forward and reverse primers, and 1.5 mM of MgCl2. PCR temperature program included 30 cycles of denaturation at 97 °C for 1 min, annealing at 60 °C for 1 min, and extension at 72 °C for 1 min. Sanger sequencing was performed with the BigDye Terminator Cycle Sequencing kit (Applied Biosystems, Foster City, CA), adding about 15 ng of template DNA in each reaction and using a temperature program that included 25 cycles of denaturation at 97 °C for 30 s, annealing at 50 °C for 15 s, and extension at 60 °C for 4 min. Samples were analyzed in a 3130 Genetic Analyzer (Applied Biosystems). Mutant and wild type (NM_000177.4; NP_000168.1) GSN sequence traces were manually compared. In addition, four healthy relatives (individuals II-1, II-9, II-10, and III-3 in Figure 1) were genotyped as indicated.

Next-generation sequencing: Next-generation sequencing (NGS) library preparation and enrichment were performed using the Illumina TruSight One Inherited Disease Panel (Illumina, San Diego, CA). Briefly, DNA was enzymatically fragmented and purified. Index adaptors were ligated to the 5′ and 3′ ends for subsequent amplification. Amplified fragments were hybridized to the Illumina TruSight One Inherited Disease Panel that enables the enrichment of 4,811 genes associated with monogenic diseases. The captured library was then purified, reamplified, and subsequently sequenced on a MiSeq platform (Illumina) using a MiSeq V3 Reagent Kit. Sequence reads were mapped to the reference human genome using Burrows-Wheeler aligner (BWA), and variant calling was performed using the GATK Unified Genotyper [28,29]. The allele frequency of the variants was annotated with public single nucleotide polymorphisms (SNP) databases (Single Nucleotide Polymorphism Database [dbSNP], 1000 Genomes, ESP6500SI, ExAC, and Genome Aggregation Database [gnomAD Browser]) and with data from more than 200 in-house exomes. Variants with an allele frequency greater than or equal to 0.1% of the genomes in the 1000 Genomes project or greater than or equal to 0.1% of the exomes included in NHLBI ESP and ExAC were excluded [30]. Variants that were considered pathogenic, possibly pathogenic, or disease-associated according to HGMD or

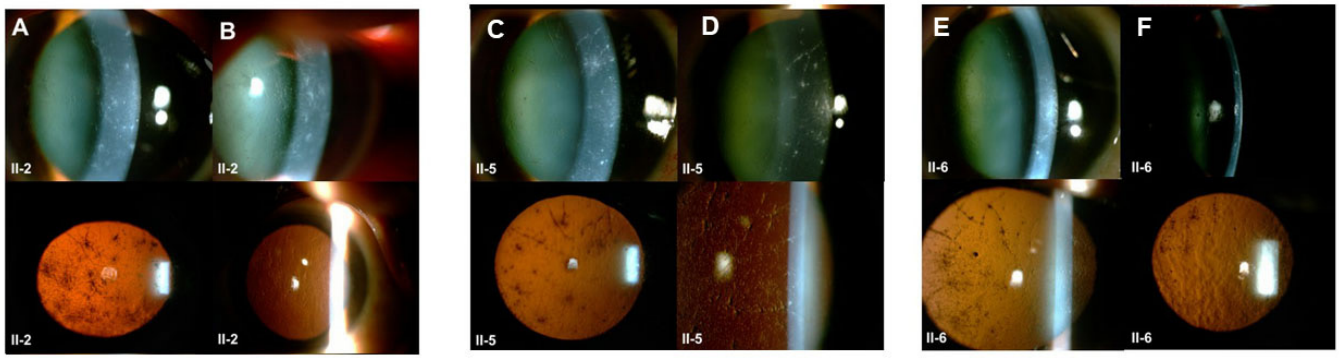

Figure 3. Slit-lamp photographs of affected subjects II-2, II-5, and II-6. Multiple central and peripheral lattice-pattern lines and thin dots with centripetal distribution are evident at the subepithelium and anterior corneal stroma. On retroillumination, branching refractile lines were evident in all three patients. **A**: Right eye. **B**: Left eye.

resulted in a frameshift, in-frame indel, stop codon change, missense mutation, or splicing-site variant were retained.

In silico analyses for pathogenicity and protein stability: In silico prediction programs, such as Polymorphism Phenotyping v2 (PolyPhen-2) [31], Sorting Intolerant From Tolerant (SIFT) [32], MutationTaster [33], and Protein Variation Effect Analyzer (PROVEAN) [34], were employed for variant pathogenicity prediction. Additionally, the DUET, Site Directed Mutator (SDM), and Cologne University Protein Stability Analysis Tool (CUPSAT) servers were used to predict the effect of the identified amino acid replacement on protein stability. DUET is an integrated computational approach for predicting effects of missense mutations on protein stability [35]. CUPSAT is a predictive tool that uses amino acid-atom potentials and torsion angle distribution to assess the amino acid environment of the mutation site [36]. SDM is a computational method that analyzes the variation of amino acid replacements occurring in a specific structural

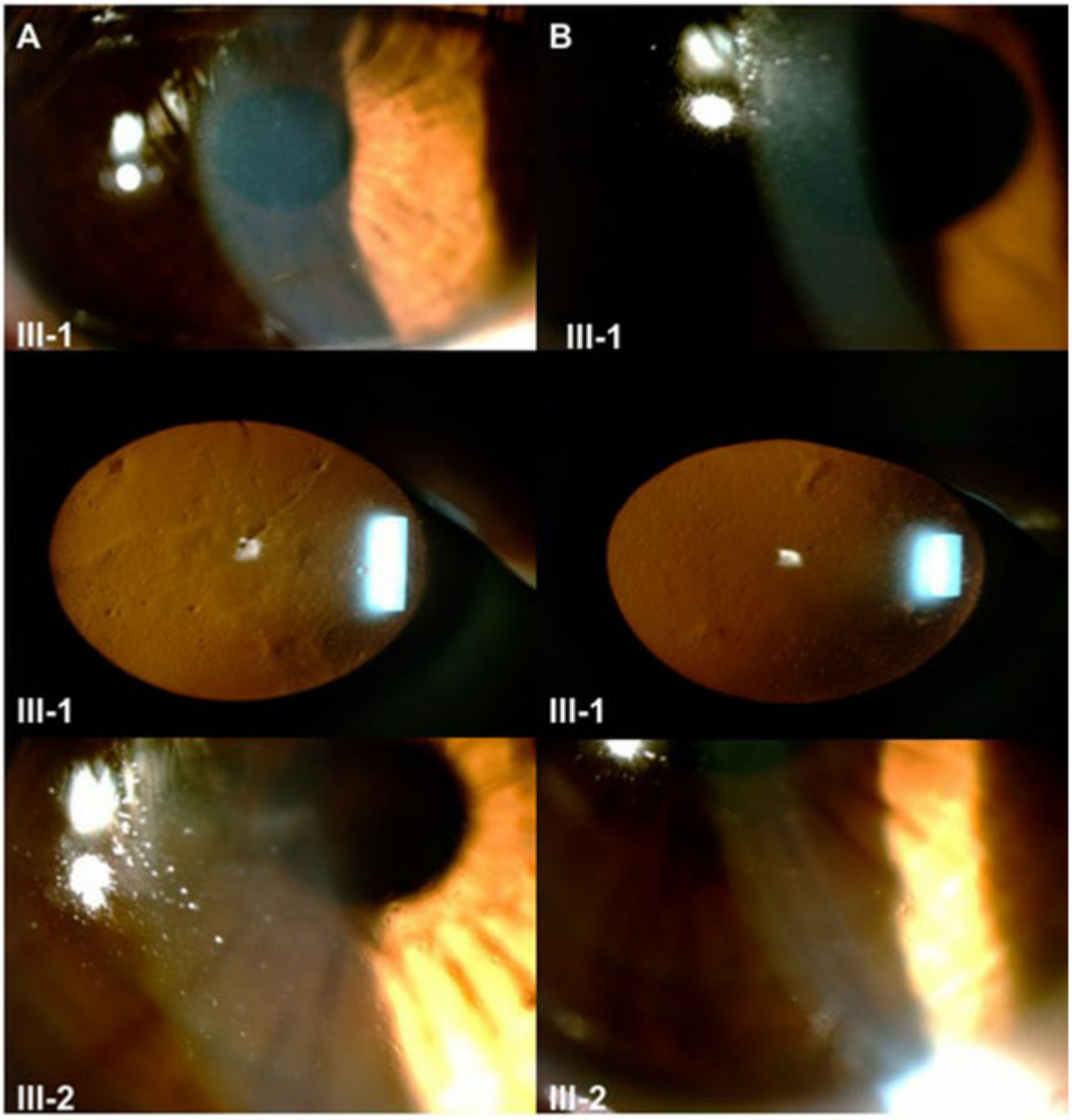

Figure 4. Slit-lamp photographs of subjects III-1 and III-2. Incipient corneal changes corresponding to lattice lines are observed predominantly in the right eye of both subjects. **A**: Right eye. **B**: Left eye.

environment that are tolerated within the family of homologous proteins of known three-dimensional (3D) structures and converts them into substitution probability tables [37]. Protein stability predictions were performed using the crystal structure of calcium-free human gelsolin (available at RCSB).

RESULTS

Clinical assessment: Five affected family members in two generations (three siblings and two sons of the proband) were identified (Figure 1). The affected subjects had a long history of visual impairment and foreign body sensation in both eyes. The proband (subject II-5, Figure 1), was a 59-year-old woman who had consulted for decreased vision over the previous 20 years and drooping eyelids. At examination, cutis laxa and bilateral blepharochalasis were evident. She had a history of carpal tunnel syndrome, peripheral neuropathy, hypothyroidism, cardiac valvulopathy, and two surgical procedures for blepharochalasis correction. Subject II-2 was a 66-year-old man with a history of lumbar radiculopathy (L3, L4), moderate hearing loss, and facial cutis laxa with hyperpigmented drooping eyelids. Subject II-6 was a 58-year-old man with ischemic heart disease and arrhythmia who had complained of mild, progressive loss of vision over the previous 5 years. Facial characteristic features of FAF such as cutis laxa and masklike facies were evident in this patient. Figure 2 shows the facial appearance of subjects II-5, II-2, and II-6. On slit-lamp corneal examination, all three affected patients exhibited bilateral subepithelial haze with pronounced central and peripheral lattice-pattern lines involving the visual axis (Figure 3A–F) which are typical LCD features. Corneal surface irregularities were evident in the central cornea.

The physical examination of the younger subjects III-1 (aged 46 years) and III-2 (aged 40 years) was unremarkable with no evidence of facial skin anomalies or systemic symptoms. However, the examination of the cornea disclosed subtle changes consisting of bilateral, thin branching refractile, whitish lines and dots located subepithelially and at the anterior stroma in the central and peripheral corneas in both subjects (Figure 4). No epithelial erosions were observed, and Descemet's membrane and endothelium were healthy in all examined individuals from this pedigree.

Histopathological analysis: Histological sections stained with hematoxylin and eosin and Congo red showed thin eyelid skin with mild orthokeratotic hyperkeratosis with papillomatosis, mild inflammatory infiltrate composed of perivascular lymphocytes in the superficial dermis, and focally pigmentary incontinence. Hair follicles and dermal appendices appeared normal. The Congo red stain showed abundant deposition of amyloid material in the basement membranes of hair follicles and in blood vessel walls (Figure 5A,B).

Genetic findings: Direct Sanger sequencing of *GSN* exon 4 in DNA from the index case was negative for the typical FAF p.Asp214Asn or Tyr mutation. No pathogenic variants were

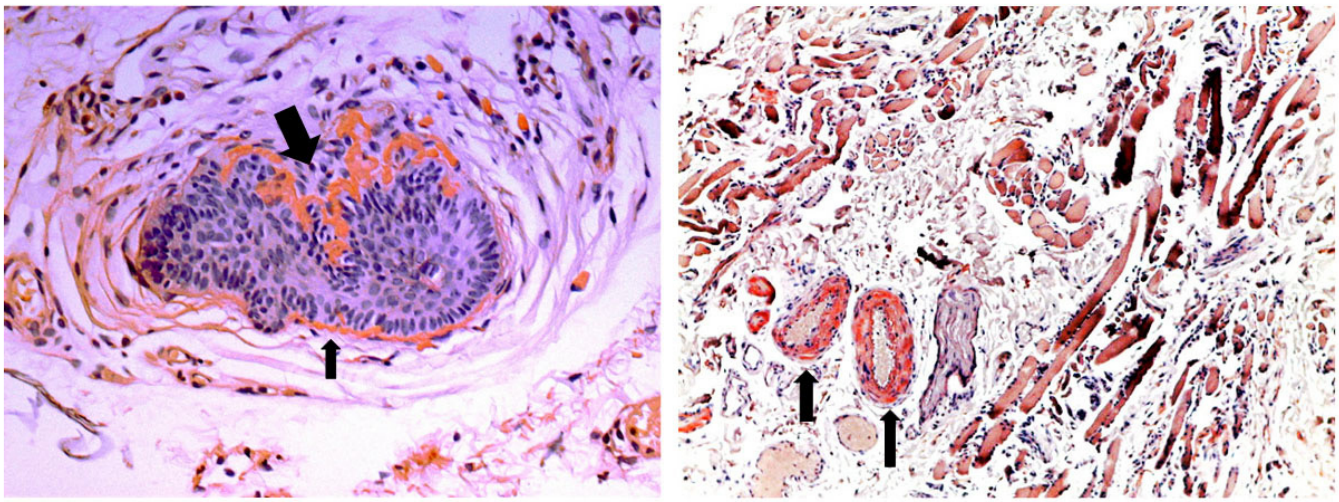

Figure 5. Histopathological findings in skin from FAF II-5 subject. **A**: Histological sections from the eyelid skin biopsy, stained with hematoxylin and eosin and Congo red, showing thin skin with mild orthokeratotic hyperkeratosis, papillomatosis, mild inflammatory infiltrate composed of perivascular lymphocytes in the superficial dermis and focally pigmentary incontinence. Dermal appendices appear normal. Congo red staining indicates amyloid deposits composed of internal degradation fragments produced during the aberrant processing in the hair follicles (arrows). **B**: Eyelid skin biopsy shows fibroconnective tissue, skeletal muscle, and vessels (arrows). The Congo red staining is positive in the walls of the vessels.

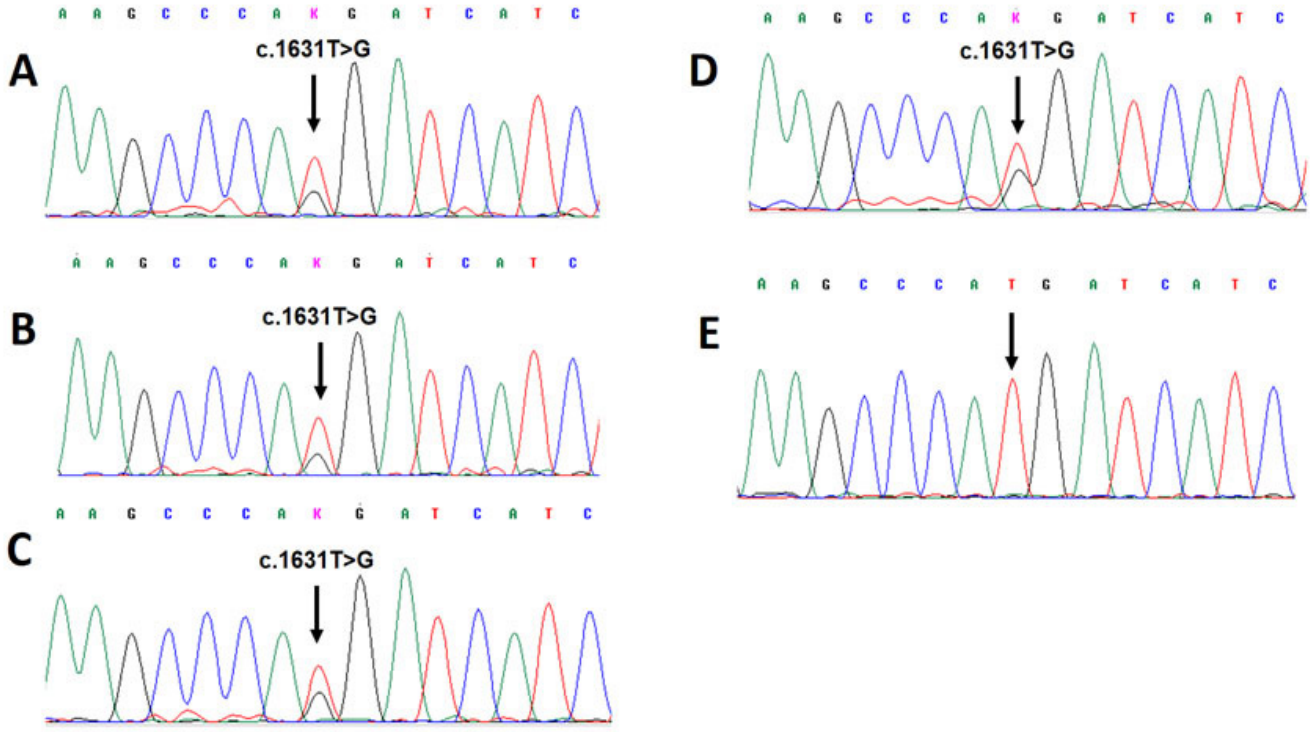

Figure 6. Partial Sanger sequencing of exon 12 of the *GSN* gene. A heterozygous T>G transversion at nucleotide 1631 was demonstrated in affected patients (**A**–**D**). This variant predicts the novel p.Met544Arg substitution at the GSN protein. **E**: A control DNA sequence is shown.

observed in the remaining sequence of this exon. Due to this result, NGS was employed for analyzing the coding regions of 4,811 genes. Next-generation sequencing of the index case (individual II-5) provided adequate coverage of the clinical exome (94.9% of the targeted regions were covered at least 20X, and 80% had at least 50X depth of coverage). After variant filtering, a candidate variant was identified at exon 12 of the *GSN* gene (NM_000177.4: c.1631T>G; NP_000168.1: p.Met544Arg; chr9:121326573T>G). This variant was confirmed with Sanger sequencing in DNA from all available relatives affected with FAF (Figure 6A–C), as well as in DNA from the two younger individuals with mild lattice corneal dystrophy and no evidence of systemic disease (Figure 6). The novel p.Met544Arg variant was absent from the NHLBI Exome Variant Server, dbSNP, gnomAD Browser, and 1000 Genomes databases (accessed in January 2019). Furthermore, this variant was absent in more than 200 in-house clinical exomes of Mexican origin. Four available healthy relatives (individuals II-1, II-9, II-10, and III-3 in Figure 1) were demonstrated to carry wild-type *GSN* sequences. Parametric linkage analysis in this family yielded a positive logarithm of the odds (LOD) score of 2.71 under a model of disease frequency of 0.0001, penetrance of 1.0, assuming no recombination ($\theta = 0$).

In silico analysis for pathogenicity and protein stability: Four different algorithms used in this study (SIFT, PolyPhen-2, MutationTaster, and PROVEAN) predicted that the p.Met544Arg is deleterious, possibly damaging, or disease causing (Figure 7A). Of note, by mapping the amino acid replacement to the known 3D structure of GSN (structural features), PolyPhen-2 and MutationTaster also predicted that GSN p.Met544Arg affects a potential calcium-sensitive, actin-binding region within the protein. Additionally, three different prediction tools based on changes in folding free-energy (DUET, SDM, and CUPSAT) predicted that this variant reduces the structural stability of the GSN protein (Figure 7B). Finally, the amino acid sequence comparison showed that methionine 544 is strictly conserved among GSN proteins from numerous vertebrate species (Figure 7C).

DISCUSSION

Among approximately 50 human amyloidotic diseases that arise from abnormal aggregation of proteins in tissues, FAF is a discrete autosomal dominant condition caused by

mutations in *GSN*. Since the first FAF description in three Finnish pedigrees 50 years ago [6], several dozens of patients from diverse countries have been recognized. Many of the studied patients had no Finnish ancestors, suggesting multiple FAF founders. The disease has genetic homogeneity, as all molecularly analyzed patients carry either p.Asp214Asn or p.Asp214Tyr GSN pathogenic variants reviewed in [38]. The identification of additional pathogenic GSN alleles is important for expanding the current knowledge of the genetic basis of human amyloidosis and for improving genotype–phenotype correlations. Previously, our group of work described a sporadic FAF case from Mexico that carried the common p.Asp214Asn variant in GSN [39].

In this work, we describe a Mexican FAF pedigree carrying a novel heterozygous p.Met544Arg GSN mutation. To the best of our knowledge, this is the third known FAF-causing GSN allele, and its identification indicates that defects outside GSN residue 214 can also result in systemic amyloidosis. In this family, a homogeneous phenotype characterized by cutis laxa and lattice corneal dystrophy was recognized in the three affected adult subjects. Peripheral neuropathy was also evident in one subject. The clinical picture in this pedigree is more compatible with the classical FAF phenotype, known to be associated with the Finnish type p.Asp214Asn GSN mutation.

Several lines of evidence support the pathogenicity of the novel p.Met544Arg GSN variant in this FAF pedigree, including familial segregation of the heterozygous variant; prediction of variant pathogenicity by various in silico tools, absence of the variant in public databases, such as 1000 Genomes, GnomAD, and dbSNP; absence in more than 200 in-house clinical exomes of Mexican origin; and strict conservation of the Met 544 residue among GSN proteins from different species.

The classic GSN p.Asp214Asn or Tyr missense mutation eliminates one of the four calcium binding sites located at the second domain of plasma gelsolin, significantly compromising calcium binding [40]. The novel p.Met544Arg identified in this study substitutes a highly conserved methionine at position 544, a nonpolar, sulfur-containing residue located at the fifth domain of the GSN protein, for arginine, a positively charged amino acid. According to a GSN model based on structural elements [41], the methionine at position 544 (which corresponds to methionine 517 in this model) forms part of a structurally variable region of the fifth domain that

A)

Algorithm	Score	Prediction
SIFT	0.000	Deleterious
PoliPhen2	1.000	Probably Damaging
MutationTaster	0.999	Disease Causing
PROVEAN	-4.479	Deleterious

B)

Algorithm	Score (ΔΔG in Kcal/mol)	Prediction
DUET	-1.628	Reduced structural Stability
SDM	-1.63	Reduced structural Stability
CUPSAT	-1.61	Reduced structural Stability

C)

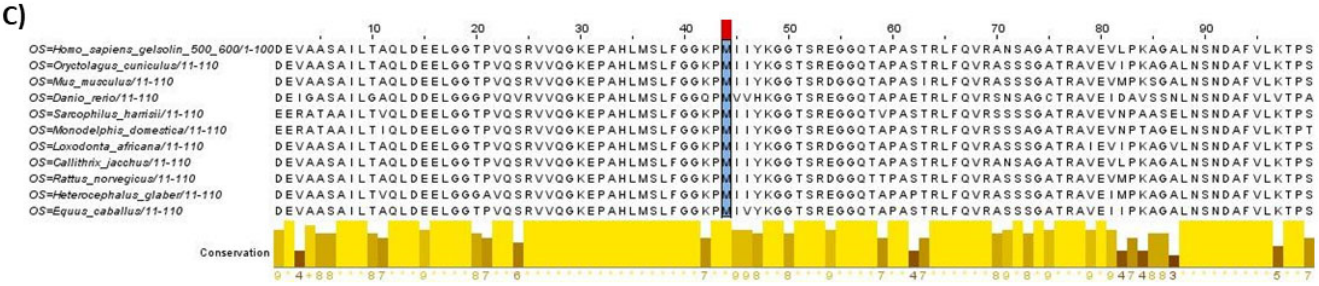

Figure 7. In silico pathogenicity predictions for the novel GSN (c.1631T>G; p.Met544Arg) variant identified in this study. **A**: Variant impact was assessed using the Sorting Intolerant From Tolerant (SIFT), Polymorphism Phenotyping v2 (PolyPhen-2), MutationTaster, and Protein Variation Effect Analyzer (PROVEAN) algorithms. **B**: In silico prediction of the effects on the protein stability produced by the p.Met544Arg replacement on GSN. Algorithm predictions are based on changes in folding free energy (ΔΔG in Kcal/mol). Protein stability predictions were performed using the crystal structure of calcium-free human gelsolin. **C**: Alignment of the amino acid sequence of gelsolin across different species. The shaded column with the red mark indicates the position of the mutated residue identified in this study. As observed, methionine 544 is strictly conserved among numerous vertebrate species.

could participate in interactions with calcium and actin. In this model, basic residues, such as arginine, near calcium ligating residues are important for creating salt bridges and performing functions such as latching or reordering of the different GSN domains [41], which might be of relevance for the p.Met544Arg variant demonstrated in this study. As additional support of the detrimental effects of this variant on protein structure, in silico prediction tools suggested that the p.Met544Arg change affects an acting binding region which is sensitive to calcium and that it reduces the structural stability of GSN.

The phenotype of this family is compatible with typical FAF, suggesting that a similar mechanism could be involved in systemic amyloidosis due to this novel GSN mutation. However, as no pathogenic variants have been reported in the fifth GSN domain, functional analyses of this region are warranted to elucidate its participation in calcium or actin binding.

In the family described here, two young relatives exhibited corneal lattice dystrophy with no evidence of skin or systemic involvement. The identification of young subjects carrying FAF-causing GSN alleles who have not developed the full clinical picture provides an opportunity for preventing systemic amyloid deposition. Although such therapy is currently unavailable, important advances in the field have been recently published [42,43], anticipating that a therapy for blocking or delaying human amyloid deposition could be developed in the next few years.

Recently, a pathogenic c.1375C>G variant located at exon 10 and resulting in a p.Pro459Arg replacement was identified in an adult subject of African descent with a postmortem diagnosis of gelsolin amyloidosis [44]. However, as this patient did not exhibit the common manifestations of cutis laxa or corneal lattice dystrophy a FAF diagnosis is debatable. Similarly, a c.100dupG predicting a frameshifting p.Ala34fs variant at the protein level was reported in a Chinese FAF familial case with an unusual severe brain phenotype [45].

In conclusion, the present results expand the molecular spectrum of FAF by identifying a novel missense variant located at the fourth GSN domain. Functional studies will be needed to recognize the mechanism by which this amino acid replacement results in systemic amyloid deposition.

REFERENCES

1. Benson MD. Inherited amyloidosis. J Med Genet 1991; 28:73-8. [PMID: 1848299].
2. Munier FL, Korvatska E, Djemai A, Le Paslier D, Zografos L, Pescia G, Schorderet DF. Kerato-epithelin mutations in four 5q31-linked corneal dystrophies. Nat Genet 1997; 15:247-51. [PMID: 9054935].
3. Yamamoto S, Okada M, Tsujikawa M, Shimomura Y, Nishida K, Inoue Y, Watababe H, Maeda N, Kurahashi H, Kinoshita S, Nakamura Y, Tano Y. A kerato-epithelin (betaig-h3) mutation in lattice corneal dystrophy type IIIA. Am J Hum Genet 1998; 62:719-22. [PMID: 9497262].
4. Stewart H, Black GC, Donnai D, Bonshek RE, McCarthy J, Morgan S, Dixon MJ, Ridgway AA. A mutation within exon 14 of the TGFBI (BIGH3) gene on chromosome 5q31 causes an asymmetric, late-onset form of lattice corneal dystrophy. Ophthalmology 1999; 106:964-70. [PMID: 10328397].
5. Kivela T, Tarkkanen A, Frangione B, Ghiso J, Haltia M. Ocular amyloid deposition in familial amyloidosis, Finnish: an analysis of native and variant gelsolin in Meretoja's syndrome. Invest Ophthalmol Vis Sci 1994; 35:3759-69. [PMID: 8088963].
6. Meretoja J. Familial systemic paramyloidosis with lattice dystrophy of the cornea, progressive cranial neuropathy, skin changes and various internal symptoms. A previously unrecognized heritable syndrome. Ann Clin Res 1969; 1:314-24. [PMID: 4313418].
7. Kiuru S. Gelsolin-related familial amyloidosis, Finnish type (FAF), and its variants found worldwide. Amyloid 1998; 5:55-66. [PMID: 9547007].
8. Purcell JJ Jr, Rodrigues M, Chishti MI, Riner RN, Dooley JM. Lattice corneal dystrophy associated with familial systemic amyloidosis (Meretoja's syndrome). Ophthalmology 1983; 90:1512-7. [PMID: 6610849].
9. Starck T, Kenyon KR, Hanninen LA, Beyer-Machule C, Fabian R, Gorn RA, McMullan FD, Baum J, McAdam KP. Clinical and histopathologic studies of two families with lattice corneal dystrophy and familial systemic amyloidosis (Meretoja syndrome). Ophthalmology 1991; 98:1197-206. [PMID: 1923356].
10. Gorevic PD, Munoz PC, Gorgone G, Purcell JJ Jr, Rodriguez M, Ghiso J, Levy E, Haltia M, Frangione B. Amyloidosis due to a mutation of the gelsolin gene in an American family with lattice corneal dystrophy type II. N Engl J Med 1991; 325:1780-5. [PMID: 1658654].
11. de la Chapelle A, Tolvanen R, Boysen G, Santavy J, Bleeker-Wagemakers L, Maury CP, Kere J. Gelsolin-derived familial amyloidosis caused by asparagine or tyrosine substitution for aspartic acid at residue 187. Nat Genet 1992; 2:157-60. [PMID: 1338910].
12. Sunada Y, Shimizu T, Mannen T, Kanazawa I. Familial amyloidotic polyneuropathy type IV (Finnish type)–the first description of a large kindred in Japan]. Rinsho Shinkeigaku 1992; 32:826-33. [PMID: 1337023].
13. Stewart HS, Parveen R, Ridgway AE, Bonshek R, Black GC. Late onset lattice corneal dystrophy with systemic familial amyloidosis, amyloidosis V, in an English family. Br J Ophthalmol 2000; 84:390-4. [PMID: 10729296].

14. Rothstein A, Auran JD, Wittpenn JR, Koester CJ, Florakis GJ. Confocal microscopy in Meretoja syndrome. Cornea 2002; 21:364-7. [PMID: 11973384].

15. Chastan N, Baert-Desurmont S, Saugier-Veber P, Dérumeaux G, Cabot A, Frébourg T, Hannequin D. Cardiac conduction alterations in a French family with amyloidosis of the Finnish type with the p.Asp187Tyr mutation in the GSN gene. Muscle Nerve 2006; 33:113-9. [PMID: 16258946].

16. Conceicao I, Sales-Luis ML, De Carvalho M, Evangelista T, Fernandes R, Paunio T, Kangas H, Coutinho P, Neves C, Saraiva MJ. Gelsolin-related familial amyloidosis, Finnish type, in a Portuguese family: clinical and neurophysiological studies. Muscle Nerve 2003; 28:715-21. [PMID: 14639586].

17. Huerva V, Velasco A, Sanchez MC, Mateo AJ, Matías-Guiu X. Lattice corneal dystrophy type II: clinical, pathologic, and molecular study in a Spanish family. Eur J Ophthalmol 2007; 17:424-9. [PMID: 17534828].

18. Ardalan MR, Shoja MM, Kiuru-Enari S. Amyloidosis-related nephrotic syndrome due to a G654A gelsolin mutation: the first report from the Middle East. Nephrol Dial Transplant 2007; 22:272-5. [PMID: 16998221].

19. Bürmann J, Fassbender K, Henn W, Lohse P, Holzhoffer C, Fassbender K, Dillmann U. Neurological manifestations of AGel amyloidosis (Meretoja's syndrome) in a German family. Fortschr Neurol Psychiatr 2011; 79:238-41. [PMID: 21480154].

20. Papathanassiou M, Liarakos VS, Vaikousis E, Paschalidis T, Agrogiannis G, Vergados I. Corneal melt in lattice corneal dystrophy type II after cataract surgery. J Cataract Refract Surg 2009; 35:185-9. [PMID: 19101443].

21. Maury CP, Liljestrom M, Boysen G, Törnroth T, de la Chapelle A, Nurmiaho-Lassila EL. Danish type gelsolin related amyloidosis: 654G-T mutation is associated with a disease pathogenetically and clinically similar to that caused by the 654G-A mutation (familial amyloidosis of the Finnish type). J Clin Pathol 2000; 53:95-9. [PMID: 10767822].

22. Solari HP, Ventura MP, Antecka E, Belfort R, Burnier MN. Danish type gelsolin-related amyloidosis in a Brazilian family: case reports. Arq Bras Oftalmol 2011; 74:286-8. [PMID: 22068858].

23. Ikeda M, Mizushima K, Fujita Y, Watanabe M, Sasaki A, Makioka K, Enoki M, Nakamura M, Otani T, Takatama M, Okamoto K. Familial amyloid polyneuropathy (Finnish type) in a Japanese family: Clinical features and immunocytochemical studies. J Neurol Sci 2007; 252:4-8. [PMID: 17097682].

24. Carrwik C, Stenevi U. Lattice corneal dystrophy, gelsolin type (Meretoja's syndrome). Acta Ophthalmol 2009; 87:813-9. [PMID: 19832730].

25. Park KJ, Park JH, Park JH, Cho EB, Kim BJ, Kim JW. The First Korean Family With Hereditary Gelsolin Amyloidosis Caused by p.D214Y Mutation in the GSN Gene. Ann Lab Med 2016; 36:259-62. [PMID: 26915616].

26. Levy E, Haltia M, Fernandez-Madrid I, Koivunen O, Ghiso J, Prelli F, Frangione B. Mutation in gelsolin gene in Finnish hereditary amyloidosis. J Exp Med 1990; 172:1865-7. [PMID: 2175344].

27. Maury CP. Homozygous familial amyloidosis, Finnish type: demonstration of glomerular gelsolin-derived amyloid and non-amyloid tubular gelsolin. Clin Nephrol 1993; 40:53-6. [PMID: 8395367].

28. Li H, Durbin R. Fast and accurate long-read alignment with Burrows-Wheeler transform. Bioinformatics 2010; 26:589-95. [PMID: 20080505].

29. McKenna A, Hanna M, Banks E, Sivachenko A, Cibulskis K, Kernytsky A, Garimella K, Altshuler D, Gabriel S, Daly M, DePristo MA. The Genome Analysis Toolkit: a MapReduce framework for analyzing next-generation DNA sequencing data. Genome Res 2010; 20:1297-303. [PMID: 20644199].

30. Lek M, Karczewski KJ, Minikel EV. Exome Aggegation Consortium. Analysis of protein-coding genetic variation in 60,706 humans. Nature 2016; 536:285-91. [PMID: 27535533].

31. Adzhubei IA, Schmidt S, Peshkin L, Ramensky VE, Gerasimova A, Bork P, Kondrashov AS, Sunyaev SR. A method and server for predicting damaging missense mutations. Nat Methods 2010; 7:248-9. [PMID: 20354512].

32. Sim NL, Kumar P, Hu J, Henikoff S, Scheneider G, Ng PC. SIFT web server: predicting effects of amino acid substitutions on proteins. Nucleic Acids Res 2012; 40:W452–7-[PMID: 22689647].

33. Schwarz JM, Cooper DN, Schuelke M, Seelow D. MutationTaster2: mutation prediction for the deep-sequencing age. Nat Methods 2014; 11:361-2. [PMID: 24681721].

34. Choi Y, Chan AP. PROVEAN web server: a tool to predict the functional effect of amino acid substitutions and indels. Bioinformatics 2015; 31:2745-7. [PMID: 25851949].

35. Pires DE, Ascher DB, Blundell TL. DUET: a server for predicting effects of mutations on protein stability using an integrated computational approach. Nucleic Acids Res 2014; 42:W314–9-[PMID: 24829462].

36. Parthiban V, Gromiha MM, Schomburg D. CUPSAT: prediction of protein stability upon point mutations. Nucleic Acids Res 2006; 34:W239–42-[PMID: 16845001].

37. Pandurangan AP, Ochoa-Montano B, Ascher DB, Blundell T. SDM: a server for predicting effects of mutations on protein stability. Nucleic Acids Res 2017; 45:W1W229–35-[PMID: 28525590].

38. Solomon JP, Page LJ, Balch WE, Kelly JW. Gelsolin amyloidosis: genetics, biochemistry, pathology and possible strategies for therapeutic intervention. Crit Rev Biochem Mol Biol 2012; 47:282-96. [PMID: 22360545].

39. Gonzalez-Rodriguez J, Ramirez-Miranda A, Hernandez-Da Mota SE, Zenteno J. TGFBI, CHST6, and GSN gene analysis in Mexican patients with stromal corneal dystrophies. Graefes Arch Clin Exp Ophthalmol 2014; 252:1267-72. [PMID: 24801599].

40. Ratnaswamy G, Huff ME, Su AI, Rion S, Kelly J. Destabilization of Ca2+-free gelsolin may not be responsible for proteolysis in Familial Amyloidosis of Finnish Type. Proc Natl Acad Sci USA 2001; 98:2334-9. [PMID: 11226240].

41. Choe H, Burtnick LD, Mejillano M, Yin HL, Robinson RC. Choe. The calcium activation of gelsolin: insights from the 3A structure of the G4–G6/actin complex. J Mol Biol 2002; 324:691-702. [PMID: 12460571].

42. Verhelle A, Nair N, Everaert I, Van Overbeke W, Supply L, Zwaenepoel O, Peleman C, Van Dorpe J, Lahoutte T, Devoogdt N, Derave W, Chuah M. VandeDriessche, Gettemans. AAV9 delivered bispecific nanobody attenuates amyloid burden in the gelsolin amyloidosis mouse model. Hum Mol Genet 2017; 26:3030-[PMID: 28605435].

43. Giorgino T, Mattioni D, Hassan A, Milani M, Mastrangelo E, Barbiroli A, Verhelle A, Gettemans J, Barzago MM, Diomede L. de Rosa. Nanobody interaction unveils structure, dynamics and proteotoxicity of the Finnish-type amyloidogenic gelsolin variant. Biochim Biophys Acta Mol Basis Dis 2019; 1865:648-60. [PMID: 30625383].

44. Oregel KZ, Shouse GP, Oster C, Martinez F, Wang J, Rosenzweig M, Deisch JK, Chen CS. Nagaraj. Atypical Presentation of Gelsolin Amyloidosis in a Man of African Descent with a Novel Mutation in the Gelsolin Gene. Am J Case Rep 2018; 19:374-81. [PMID: 29599423].

45. Feng X, Zhu H, Zhao T, Hou Y, Liu J. A new heterozygous G duplicate in exon1 (c.100dupG) of gelsolin gene causes Finnish gelsolin amyloidosis in a Chinese family. Brain Behav 2018; 8:e01151-[PMID: 30417985].

Articles are provided courtesy of Emory University and the Zhongshan Ophthalmic Center, Sun Yat-sen University, P.R. China. The print version of this article was created on 2 May 2020. This reflects all typographical corrections and errata to the article through that date. Details of any changes may be found in the online version of the article.